



A study of radiative properties of fractal soot aggregates using the superposition *T*-matrix method

Li Liu^{a,b}, Michael I. Mishchenko^{a,*}, W. Patrick Arnott^c

^a NASA Goddard Institute for Space Studies, 2880 Broadway, New York, NY 10025, USA

^b Department of Applied Physics and Applied Mathematics, Columbia University, New York, NY 10025, USA

^c Department of Physics, Mail Stop 220, University of Nevada/Reno, 1664 N Virginia St., Reno, NV 89557, USA

ARTICLE INFO

Article history:

Received 11 September 2007

Received in revised form

1 May 2008

Accepted 2 May 2008

Keywords:

Soot aggregates

Absorption cross section

Scattering cross section

Extinction cross section

Single-scattering albedo

Asymmetry parameter

Fractal dimension

ABSTRACT

We employ the numerically exact superposition *T*-matrix method to perform extensive computations of scattering and absorption properties of soot aggregates with varying state of compactness and size. The fractal dimension, D_f , is used to quantify the geometrical mass dispersion of the clusters. The optical properties of soot aggregates for a given fractal dimension are complex functions of the refractive index of the material m , the number of monomers N_s , and the monomer radius a . It is shown that for smaller values of a , the absorption cross section tends to be relatively constant when $D_f < 2$ but increases rapidly when $D_f > 2$. However, a systematic reduction in light absorption with D_f is observed for clusters with sufficiently large N_s , m , and a . The scattering cross section and single-scattering albedo increase monotonically as fractals evolve from chain-like to more densely packed morphologies, which is a strong manifestation of the increasing importance of scattering interaction among spherules. Overall, the results for soot fractals differ profoundly from those calculated for the respective volume-equivalent soot spheres as well as for the respective external mixtures of soot monomers under the assumption that there are no electromagnetic interactions between the monomers. The climate-research implications of our results are discussed.

Published by Elsevier Ltd.

1. Introduction

Soot particles form a climatically important category of tropospheric aerosols. However, their radiative effects on climate are still poorly quantified, in part due to the strong temporal and spatial variability of soot aerosols as well as because of their complex morphologies. Carbonaceous soot particles frequently exist in the form of clusters of small, nearly spherical monomers (spherules). It has been demonstrated that the overall morphology of a dry soot aerosol is well represented by a fractal cluster described by the following statistical scaling law [1,2]:

$$N_s = k_0 \left(\frac{R_g}{a} \right)^{D_f}, \quad (1)$$

where a is the monomer mean radius, k_0 is the fractal prefactor, D_f is the fractal dimension, N_s is the number of monomers in the cluster, and R_g , called the radius of gyration, is a measure of the overall cluster radius. The latter is

* Corresponding author. Tel.: +1 212 678 5590; fax: +1 212 678 5622.

E-mail address: crmim@giss.nasa.gov (M.I. Mishchenko).

defined by

$$R_g^2 = \frac{1}{N_s} \sum_{i=1}^{N_s} r_i^2, \quad (2)$$

where r_i is the distance of the i th sphere to the cluster's center of mass. The fractal dimension is important for the quantitative characterization of the aggregate morphology. Densely packed aggregates have D_f values close to 3, whereas the fractal dimension of chain-like branched clusters can be significantly smaller. The other important structural coefficient, k_0 , is also related to the state of compactness of a fractal particle. For a fixed D_f , the packing density tends to be smaller as k_0 decreases.

It is widely believed that the fractal dimension of a soot particle reflects its history and thus is controlled by the particle source, generating conditions, and aging processes [3]. Post-combustion soot exists in open chain-like structures of individual spherules [4]. As the aerosol ages, the chain-like aggregate tends to collapse into a more compact soot cluster [5,6]. The changing morphology of soot through aging is expected to have an important effect on the predicted optical characteristics [7].

As fractal aggregates are fundamentally nonspherical in shape, the traditional Lorenz–Mie theory [8] may not be applicable. Berry and Percival [9] first introduced fractal concepts to study the optics of fractal aggregates using a mean-field approximation. Since then, the calculations of light scattering and absorption by fractal aggregates with a soot-like refractive index have been performed primarily using various approximate and numerical techniques such as the Rayleigh–Gans–Debye approximation [10], the volume integral equation formulation [7], the coupled dipole method [11], and the anomalous diffraction approximation [12]. We will not discuss here the validity limits for these approaches. The interested reader is referred to the comprehensive review by Sorensen [2].

The numerically exact superposition T -matrix method has been evolving very rapidly in recent years and has been increasingly applied to the computation of electromagnetic scattering by multi-sphere clusters [8,13–19]. In this study, we employ this technique to calculate the scattering and absorption properties of fractal soot aggregates. An important goal of this research is to study the optical properties of soot aerosols as they age and evolve from chain-like structures into closely packed compact clusters. We also quantify and analyze the errors caused by employing the simple volume-equivalent-sphere model as well as the external mixing approximation frequently used in climate models to represent the scattering and absorption properties of soot aerosols.

2. Methodology

The ensemble-averaged scattering, C_{sca} , and absorption, C_{abs} , cross sections [8] are important parameters required to understand the radiative properties of ambient soot particles [20]. Other useful integral photometric characteristics include the extinction cross section, $C_{ext} = C_{abs} + C_{sca}$, the single-scattering albedo $\varpi = C_{sca}/C_{ext}$, and the asymmetry parameter g [8]. We calculate the optical properties of fractal-like soot aggregates using the efficient superposition T -matrix code developed for multi-sphere groups in random orientation. The code is documented in [21] and is publicly available on-line at <ftp://ftp.eng.auburn.edu/pub/dmckwski/scatcodes/index.html>. The critical advantages of this method are that it is numerically exact, is much more efficient than any other numerical technique based on an explicit solution of the Maxwell equations, can be applied to a wide range of particle sizes, and generates all scattering and absorption characteristics of particles necessary to interpret the results of any in situ and remote sensing observations as well as to compute the radiative energy balance.

We mainly use the cluster–cluster aggregation algorithm described by Mackowski [22] to generate random soot fractals. The basic idea of this method is to generate a sequence of random sphere positions subject to the constraint that the positions, at any point in the sequence, identically satisfy Eq. (1) for given k_0 and D_f . However, when the cluster–cluster aggregation algorithm fails to generate fractals for a certain fractal dimension value, we use the original diffusion-limited aggregation (DLA) method as described in [23], in which the algorithm starts with a pair of spheres in contact for pre-set k_0 and D_f values and adds a single monomer at a time. Compared to the original DLA algorithms, the cluster–cluster aggregation process is more realistic and requires less computer time.

With the computer algorithms to generate fractal aggregates and the superposition T -matrix method to calculate electromagnetic scattering by these multi-sphere clusters, we investigate how the radiative properties of soot aggregates change with fractal dimension. To make our study more representative, we also vary the refractive index m , the number of monomers N_s , and the monomer radius a . Specifically, we consider soot fractals with $m = 1.75 + i0.5$ and $2 + i$, $N_s = 200, 400, 600$, and 800 , $a = 15$ and 25 nm, and fractal dimensions D_f ranging from 1.25 to 3 in steps of 0.25. All calculations have been performed at the wavelength 870 nm.

In order to isolate the specific effects of the fractal dimension, it would be ideal to keep the prefactor value fixed while performing the above-described computations. However, for each value of the fractal dimension (or the prefactor), there is only a narrow range of k_0 (or D_f) values, which allow a cluster to be generated. If the k_0 or the D_f value goes outside of its respective range, the neighboring monomers may either be too close and overlap or be too far apart and not in contact. Fortunately, it is well known that the fractal dimension is the primary structural parameter [24] defining the compactness state of a fractal particle. Therefore, we have decided to ignore the potential minor effect of the requisite variation of the prefactor with D_f and attribute all morphology-caused changes in the cluster optical properties to the effects of the fractal dimension. Please note that in this study the particle mass is held constant for particles with a fixed number of monomers

Table 1
Fractal parameters used in this study

D_f	$N_s = 200$		$N_s = 400$		$N_s = 600$		$N_s = 800$	
	k_0	R_g/a	k_0	R_g/a	k_0	R_g/a	k_0	R_g/a
1.25	1.6	47.59	1.6	82.86	2	95.87	2	120.68
1.5	1.6	25.00	1.6	39.69	1.6	52.00	1.6	63.00
1.75	1.6	15.78	1.6	23.46	1.6	29.57	1.6	34.86
2	1.6	11.18	1.6	15.81	1.6	19.36	1.6	22.36
2.25	1.6	8.55	1.6	11.63	1.6	13.93	1.6	15.83
2.5	1.6	6.90	1.6	9.10	1.6	10.71	1.6	12.01
2.75	1.6	5.79	1.6	7.45	1.6	8.63	1.6	9.58
3	1.2	5.50	1.2	6.93	1.2	7.94	1.2	8.74

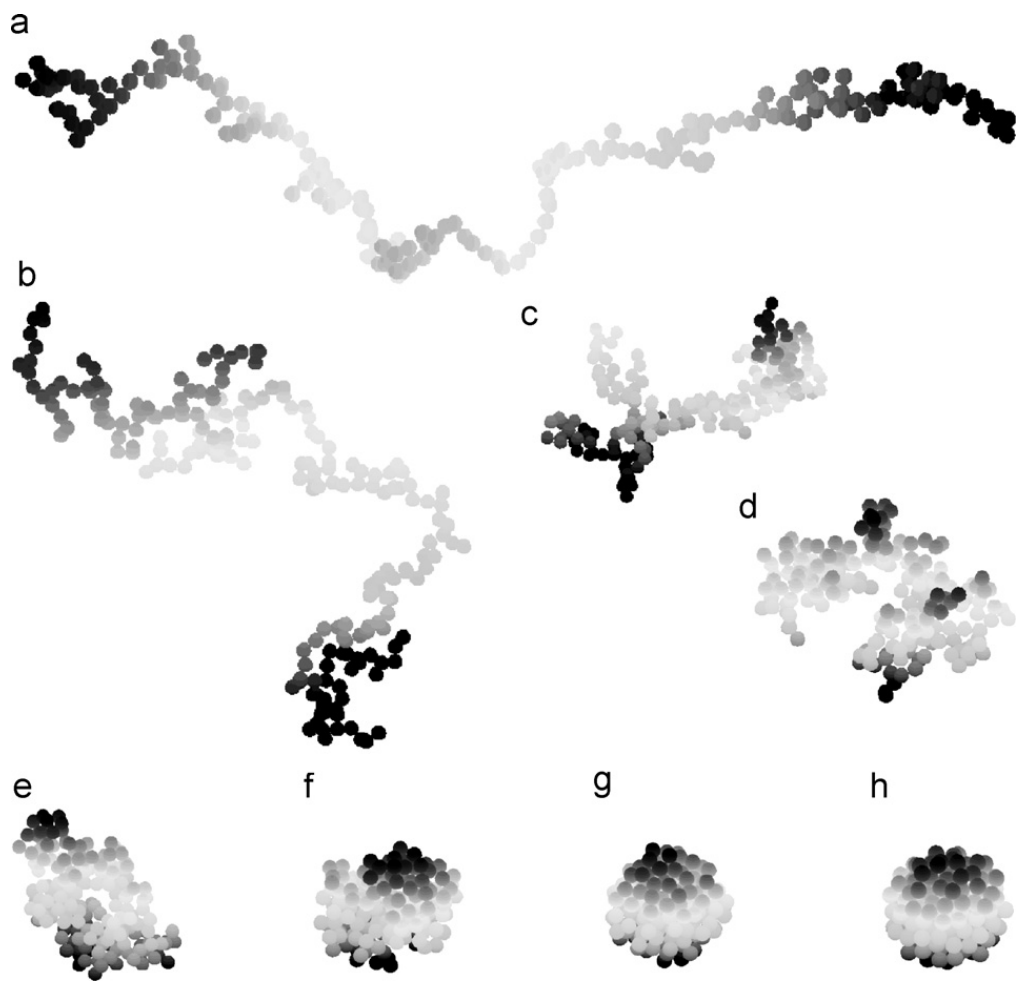


Fig. 1. Fractal aggregates composed of 200 monomers and characterized by different values of the fractal parameters D_f and k_0 . (a)–(g) $D_f = 1.25, 1.5, 1.75, 2, 2.25, 2.5, 2.75$ and $k_0 = 1.6$. (h) $D_f = 3$ and $k_0 = 1.2$.

and monomer size, while the fractal dimension is varied from 1.25 to 3, as particle shape changes from almost linear to almost spherical. The prefactor values corresponding to the above-indicated D_f values are listed in Table 1, along with the ratios of the radius of gyration relative to the monomer size.

3. Results and discussion

Fig. 1 shows the aggregates generated for various fractal dimension and prefactor values. The number of spherules is fixed at $N_s = 200$. The prefactor and fractal dimension values are pre-specified according to Table 1. Obviously, the aggregates become more compact as D_f increases.

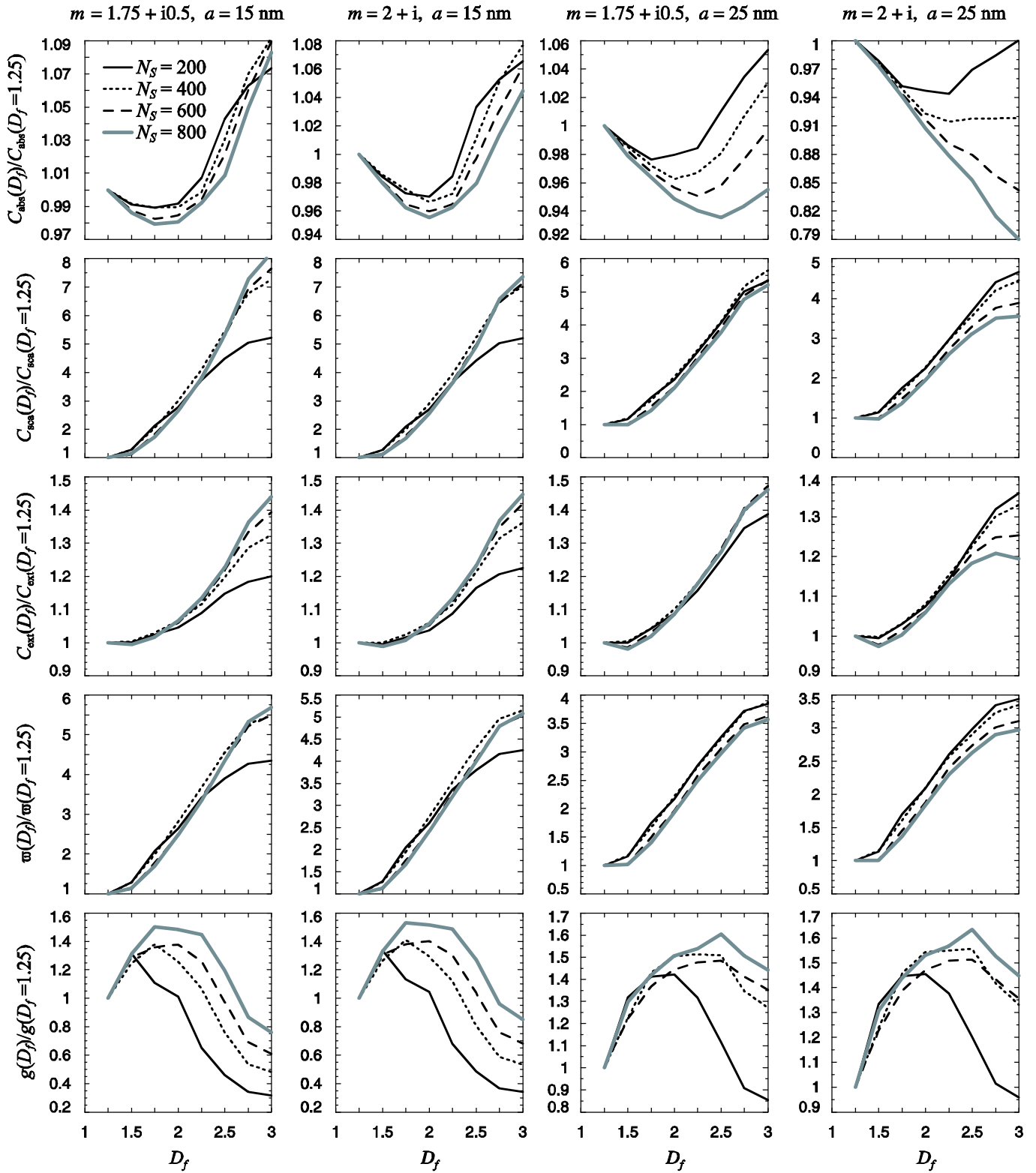


Fig. 2. Integral optical characteristics of different fractal soot aggregates as functions of fractal dimension.

Fig. 2 depicts the optical cross sections, the single-scattering albedo, and the asymmetry parameter for different soot aggregates as functions of the fractal dimension. These integral photometric characteristics are normalized by the corresponding values calculated for $D_f = 1.25$ and tabulated in Table 2. From left to right are the results calculated for the refractive index $m = 1.75 + i0.5$ and monomer radius $a = 15$ nm (column 1); $m = 2 + i$ and $a = 15$ nm (column 2); $m = 1.75 + i0.5$ and $a = 25$ nm (column 3); and $m = 2 + i$ and $a = 25$ nm (column 4). The solid black, dotted, dashed, and solid gray curves depict the results computed for fractals with the numbers of monomers $N_s = 200, 400, 600$, and 800 , respectively.

Table 2Integral photometric characteristics of soot clusters calculated for $D_f = 1.25$

m	a (nm)	N_s	$C_{abs} (\mu m^2)$	$C_{sca} (\mu m^2)$	$C_{ext} (\mu m^2)$	ϖ	g
1.75+i0.5	15	200	1.428×10^{-2}	4.478×10^{-4}	1.473×10^{-2}	3.040×10^{-2}	0.357
		400	2.857×10^{-2}	1.121×10^{-3}	2.970×10^{-2}	3.774×10^{-2}	0.385
		600	4.294×10^{-2}	2.083×10^{-3}	4.503×10^{-2}	4.626×10^{-2}	0.415
		800	5.723×10^{-2}	3.032×10^{-3}	6.026×10^{-2}	5.031×10^{-2}	0.417
	25	200	6.785×10^{-2}	5.754×10^{-3}	7.361×10^{-2}	7.817×10^{-2}	0.415
		400	0.136	1.397×10^{-2}	0.149	9.343×10^{-2}	0.443
		600	0.203	2.496×10^{-2}	0.228	0.109	0.486
		800	0.271	3.648×10^{-2}	0.307	0.119	0.480
2+i	15	200	2.389×10^{-2}	9.616×10^{-4}	2.485×10^{-2}	3.870×10^{-2}	0.350
		400	4.767×10^{-2}	2.406×10^{-3}	5.007×10^{-2}	4.806×10^{-2}	0.377
		600	7.162×10^{-2}	4.449×10^{-3}	7.607×10^{-2}	5.849×10^{-2}	0.409
		800	9.522×10^{-2}	6.488×10^{-3}	1.017×10^{-1}	6.379×10^{-2}	0.411
	25	200	0.114	1.231×10^{-2}	0.126	9.765×10^{-2}	0.408
		400	0.226	2.974×10^{-2}	0.256	0.116	0.437
		600	0.338	5.266×10^{-2}	0.391	0.135	0.481
		800	0.449	7.689×10^{-2}	0.525	0.146	0.477

It can be seen from Fig. 2 that when a soot particle is moderately absorbing and the monomer size is small (i.e., $m = 1.75+i0.5$ and $a = 15$ nm), the absorption cross section is not a sensitive function of the fractal dimension when $D_f < 2$, but increases dramatically when $D_f > 2$. This can be due to a large average monomer separation in chain-like aggregates, which makes the electromagnetic interactions between the monomers weaker. When $D_f > 2$, the intensifying interaction between spherules serves to increase the probability of absorption.

The absorption cross sections gradually decrease with increasing fractal dimension, reach minimal values for D_f around 2, and then increase rather rapidly when $D_f > 2$ for the aggregates composed of more absorptive spherules of the same size (i.e., $m = 2+i$ and $a = 15$ nm). A similar pattern is also observed for the clusters with $m = 1.75+i0.5$ and $a = 25$ nm. The underlying reason for this pattern may be the competition of two effects. On one hand, $C_{abs}(D_f)$ tends to decrease with increasing fractal dimension for chain-like clusters since less and less of the absorbing material becomes directly exposed to the incident radiation. Eventually, however, the growing interaction among monomers increases the probability of light absorption, thereby resulting in larger $C_{abs}(D_f)/C_{abs}(D_f = 1.25)$ ratios. For the fractals with $m = 2+i$, $a = 25$ nm, and $N_s = 600$ and 800, the effect of increasing fractal compactness is always to decrease the absorption cross section. This may be caused by a shielding effect of the outer layer of monomers, which blocks light from penetrating deeply inside the compact fractal.

The orientation-averaged scattering cross section, on the other hand, increases monotonically with fractal dimension, thus implying the intensifying scattering interaction between the spherules as fractals age. The same is also true of the single-scattering albedo. The asymmetry parameter is mostly determined by the cluster size and morphology and does not depend much on the soot refractive index.

In a similar vein, Fig. 3 depicts the ratios of C_{abs} , C_{sca} , C_{ext} , ϖ , and g computed for fractal aggregates to those for the corresponding external mixtures predicted by the Lorenz–Mie theory, assuming that there are no electromagnetic interactions between the monomers. Clustering results in a rather significant enhancement, up to $\sim 41\%$, in absorption relative to the case of independently scattering spherules. The enhancement of absorption does not appear to be a sensitive function of N_s for fractals with $m = 1.75+i0.5$ and $a = 15$ nm. For $m = 2+i$, $a = 25$ nm, and $N_s = 800$, the absorption enhancement decreases from $\sim 30\%$ to 2% with increasing compactness. The most profound effects of aggregation are on the scattering cross section, the single-scattering albedo, and the asymmetry parameter, for which the relative enhancement ratios can exceed two orders of magnitude. This is not surprising because both ϖ and g are very close to zero for the individual small spherules, which is a typical trait of absorbing Rayleigh spheres, whilst the single-scattering albedo and the asymmetry parameter for the aggregates have values representative of wavelength-sized or larger scatterers.

The integral photometric properties of the clusters are also significantly different from those of the volume-equivalent homogenous spheres, as shown in Fig. 4. This is especially true of the scattering cross section, single-scattering albedo, and asymmetry parameter. Not surprisingly, the overall differences in the scattering cross section between the aggregates and the corresponding equal-volume spheres become smaller for compact aggregates with D_f close to 3. The likely explanation of why the results do not exactly approach those for an equivalent-volume sphere could be that aggregates still have empty spaces in them even when the fractal dimension value is close to 3.

4. Summary and future work

In summary, our analysis of the numerically exact T -matrix results demonstrates that the fractal dimension is a very important morphological parameter for the evaluation of the optical properties of a soot cluster. Scattering

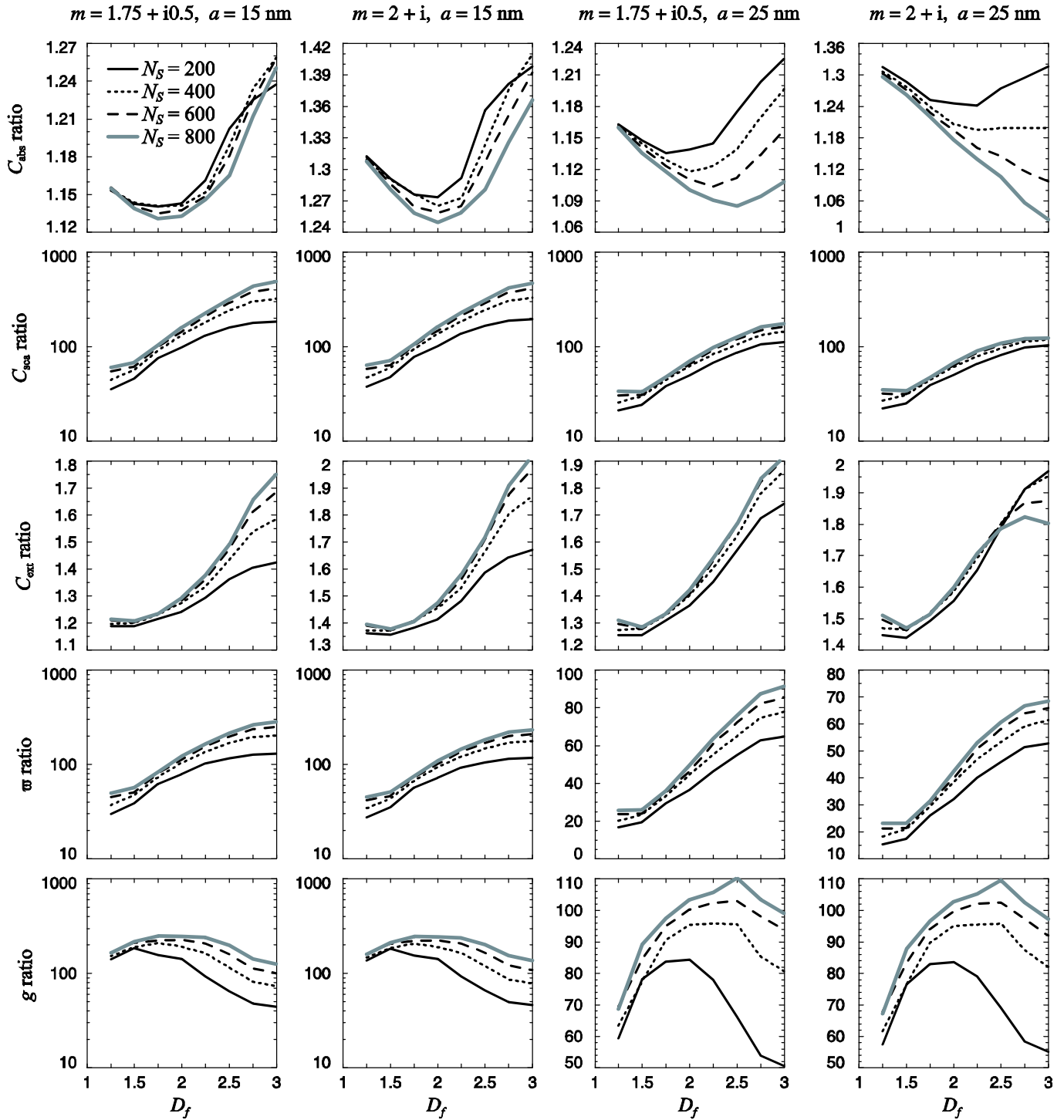


Fig. 3. Ratios of the integral photometric characteristics of soot fractals to those computed using the external-mixing approximation.

interactions among spherules are important even for chain-like structures, in which spherules are separated by large average distances, and becomes even more important as fluffy clusters age and collapse to form closely packed compact structures. Our findings do not necessarily support those by Berry and Percival [9] who used an approximate mean-field theory and concluded that absorption by aggregates is not significantly affected by multiple scattering among spherules when $D_f < 2$. The actual relationship between the absorption cross section and the fractal dimension is a complex function of the refractive index, the number of monomers, and the monomer size.

The results for a soot cluster can differ fundamentally from those calculated for two models commonly used in climate modeling, viz., the respective volume-equivalent soot sphere and the external mixture of soot spherules. This indicates that the complex morphology of dry soot aerosols must be explicitly taken into account in climate radiation balance

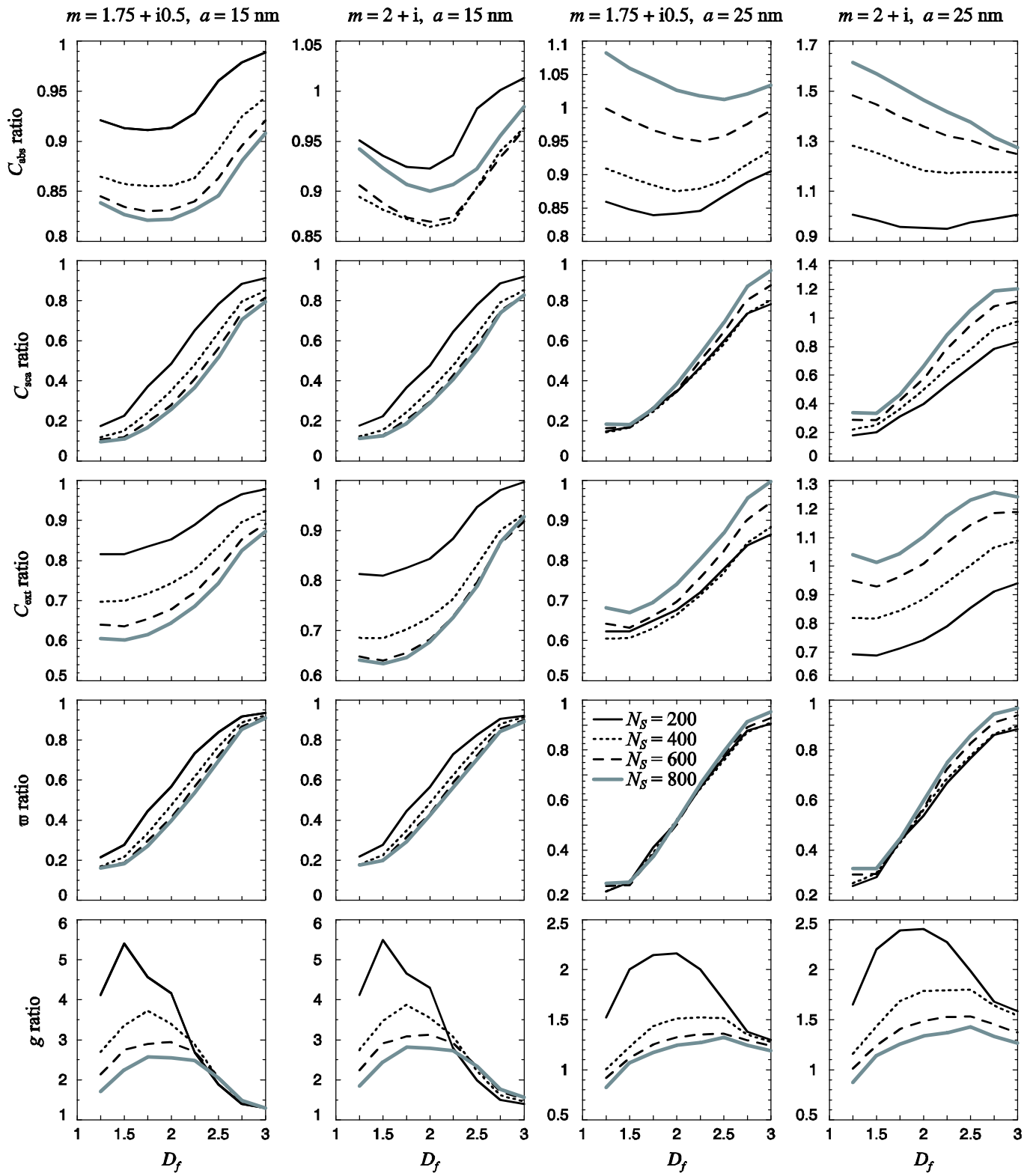


Fig. 4. Ratios of the integral photometric characteristics of soot fractals to those computed for the respective volume-equivalent spheres.

applications. Our results are also important for optical diagnostics of combustion-generated soot aggregates as well as atmospheric measurements of light absorption using the photoacoustic method [25,26].

Our conclusions are based on computations of electromagnetic scattering and absorption for only one realization of a cluster for the specified fractal parameters, whereas there is an infinite diversity of specific geometrical configurations for given fractal dimension and prefactor values. However, our previous study [16] showed that the optical properties of only one realization of a soot cluster rendered by the fractal-particle generator [22,23] for given D_f and k_0 can adequately

represent the properties of the entire ensemble of fractal-parameter-equivalent soot clusters. Thus the conclusions drawn in this study are rather general and apply equally to ensembles of soot clusters.

Finally we note that during the aging process, soot particles can aggregate with hydrophilic particles or acquire coatings of other aerosol species [3], or they can become internally mixed [27]. It is, therefore, important to parallel this study by a theoretical analysis of electromagnetic scattering and absorption by internally mixed aerosols and aerosols with a coating.

Acknowledgments

We thank Dan Mackowski for providing his code for the computer generation of fractal clusters consisting of hard spheres and an anonymous reviewer for helpful comments on the initial manuscript. This research was funded by the NASA Radiation Sciences Program managed by Hal Maring, by the NASA Glory Mission Project, and by the Department of Energy Atmospheric Sciences Program.

References

- [1] Mikhailov EF, Vlasenko SS, Kiselev AA. Optics and structure of carbonaceous soot aggregates. In: Markel VA, George TF, editors. Optics of nanostructured materials. Hoboken, NJ: John Wiley; 2001. p. 413–66.
- [2] Sorensen CM. Light scattering by fractal aggregates: a review. *Aerosol Sci Technol* 2001;35:648–87.
- [3] Adachi K, Chung SH, Friedrich H, Buseck PR. Fractal parameters of individual soot particles determined using electron tomography: implications for optical properties. *J Geophys Res* 2007;112:D14202.
- [4] Abel SJ, Haywood JM, Highwood EJ, Li J, Buseck PR. Evolution of biomass burning aerosol properties from an agricultural fire in southern Africa. *Geophys Res Lett* 2003;30:1783.
- [5] Johnson DW, Kilsby CG, McKenna DS, Saunders RW, Jenkins GJ, Smith FB, et al. Airborne observations of the physical and chemical characteristics of the Kuwait oil smoke plume. *Nature* 1991;353:617–21.
- [6] Reid JS, Hobbs PV. Physical and optical properties of young smoke from individual biomass fires in Brazil. *J Geophys Res* 1998;103:32013–30.
- [7] Chen HY, Iskander MF, Penner JE. Light scattering and absorption by fractal agglomerates and coagulations of smoke aerosols. *J Mod Opt* 1990;37:171–81.
- [8] Mishchenko MI, Travis LD, Lacis AA. Scattering, absorption, and emission of light by small particles. Cambridge: Cambridge University Press; 2002. Available on-line at <<http://www.giss.nasa.gov/~crmim/books.html>>.
- [9] Berry MV, Percival IC. Optics of fractal clusters such as smoke. *Opt Acta* 1986;33:577–91.
- [10] Mountain RD, Mulholland GW. Light scattering from simulated smoke agglomerates. *Langmuir* 1988;4:1321–6.
- [11] Singham SB, Bohren CF. Scattering of unpolarized and polarized light by particle aggregates of different size and fractal dimension. *Langmuir* 1993;9:1431–5.
- [12] Khlebtsov NG. Optics of fractal clusters in the anomalous diffraction approximation. *J Mod Opt* 1993;40:2221–35.
- [13] Mackowski DW. Calculation of total cross sections of multiple-sphere clusters. *J Opt Soc Am A* 1994;11:2851–61.
- [14] Fuller KA, Malm WC, Kreidenweis SM. Effects of mixing on extinction by carbonaceous particles. *J Geophys Res* 1999;104:15941–54.
- [15] Liu L, Mishchenko MI. Effects of aggregation on scattering and radiative properties of soot aerosols. *J Geophys Res* 2005;110:D11211.
- [16] Liu L, Mishchenko MI. Scattering and radiative properties of complex soot and soot-containing aggregate particles. *QSRT* 2007;106:262–73.
- [17] Mishchenko MI, Videen G, Babenko VA, Khlebtsov NG, Wriedt T. *T*-matrix theory of electromagnetic scattering by particles and its applications: a comprehensive reference database. *QSRT* 2004;88:357–406.
- [18] Mishchenko MI, Videen G, Babenko VA, Khlebtsov NG, Wriedt T. Comprehensive *T*-matrix reference database: a 2004–06 update. *QSRT* 2007;106:304–24.
- [19] Mishchenko MI, Videen G, Khlebtsov NG, Wriedt T, Zakharova NT. Comprehensive *T*-matrix reference database: A 2006–07 update. *QSRT* 2008;109:1447–60.
- [20] Hansen JE, Sato M, Ruedy R. Radiative forcing and climate response. *J Geophys Res* 1997;102:6831–64.
- [21] Mackowski DW, Mishchenko MI. Calculation of the *T* matrix and the scattering matrix for ensembles of spheres. *J Opt Soc Am A* 1996;13:2266–78.
- [22] Mackowski DW. A simplified model to predict the effects of aggregation on the absorption properties of soot particles. *QSRT* 2006;100:237–49.
- [23] Mackowski DW. Electrostatics analysis of radiative absorption by sphere clusters in the Rayleigh limit: application to soot particles. *Appl Opt* 1995;34:3535–45.
- [24] Mulholland GW, Bohren CF, Fuller KA. Light scattering by agglomerates: coupled electric and magnetic dipole method. *Langmuir* 1994;10:2533–46.
- [25] Arnott WP, Moosmüller H, Sheridan PJ, et al. Photoacoustic and filter-based ambient aerosol light absorption measurements: instrument comparisons and the role of relative humidity. *J Geophys Res* 2003;108:4034.
- [26] Raspet R, Slaton WV, Arnott WP, Moosmüller H. Evaporation–condensation effects on resonant photoacoustics of volatile aerosols. *J Atmos Oceanic Technol* 2003;20:685–95.
- [27] Pósfai M, Simons R, Li J, Hobbs PV, Buseck PR. Individual aerosol particles from biomass burning in southern Africa: 1. Compositions and size distributions of carbonaceous particles. *J Geophys Res* 2003;108:8483.